ANTHROPOLOGY

Footprint evidence for locomotor diversity and shared habitats among early Pleistocene hominins

Kevin G. Hatala[1,2]*, Neil T. Roach[3], Anna K. Behrensmeyer[4], Peter L. Falkingham[5], Stephen M. Gatesy[6], Erin Marie Williams-Hatala[1,2,7], Craig S. Feibel[8,9], Ibrae Dalacha[10], Martin Kirinya[10], Ezekiel Linga[10], Richard Loki[10], Apolo Alkoro Longaye[10], Malmalo Longaye[10], Emmanuel Lonyericho[10], Iyole Loyapan[10], Nyiber Nakudo[10], Cyprian Nyete[10], Louise N. Leakey[10,11]

For much of the Pliocene and Pleistocene, multiple hominin species coexisted in the same regions of eastern and southern Africa. Due to the limitations of the skeletal fossil record, questions regarding their interspecific interactions remain unanswered. We report the discovery of footprints (~1.5 million years old) from Koobi Fora, Kenya, that provide the first evidence of two different patterns of Pleistocene hominin bipedalism appearing on the same footprint surface. New analyses show that this is observed repeatedly across multiple contemporaneous sites in the eastern Turkana Basin. These data indicate a sympatric relationship between *Homo erectus* and *Paranthropus boisei*, suggesting that lake margin habitats were important to both species and highlighting the possible influence of varying levels of coexistence, competition, and niche partitioning in human evolution.

The fossil record provides evidence that multiple hominin species coexisted at the same times in the same regions of eastern and southern Africa (*1*). Co-occurrence of closely related taxa in the same ecosystems is often explained by adaptive niche partitioning, in which disparate morphological and behavioral adaptations limit direct competition by allowing species to access different resources within their shared landscape (*2*, *3*). However, hypothesized hominin sympatry is typically based on co-occurrence of skeletal fossils within deposits that span tens to hundreds of square kilometers, and that accumulated over thousands to tens of thousands of years (*4*, *5*). The spatiotemporal resolution of these data is not sufficient to determine whether species inhabited the same landscapes at the same time (within years to decades), nor is it sufficient to address the potential role of interspecific competition in human evolution, including in the emergence of our own genus (*6*).

Beyond the spatiotemporal limitations of skeletal fossils that constrain what we know about hominin sympatry, we also have limited knowledge regarding adaptive divergences between contemporaneous taxa, including *Homo erectus* and *Paranthropus boisei* (*7*, *8*). Much work has focused on hypothesized dietary differences (*9*–*12*) because most fossils confidently attributed to these taxa are cranial and dental remains (*7*). One hypothesis posits that *H. erectus* was the earliest hominin to practice fully modern human-like bipedal walking and endurance running, and that this adaptation set them on a different evolutionary trajectory (*13*). With a sparse record of postcranial fossils that are mostly isolated, fragmentary, and/or difficult to attribute taxonomically, there is little skeletal evidence allowing direct comparisons of bipedalism in *H. erectus* and *P. boisei* (*14*, *15*).

The early Pleistocene deposits of the Turkana Basin in northern Kenya provide new evidence regarding sympatric relationships between *H. erectus* and *P. boisei* (*7*, *8*). We present the discovery of an early Pleistocene footprint site in the upper KBS Member of the Koobi Fora Formation (*16*). We analyze the hominin footprints and re-examine an extensive suite of track assemblages of similar age in the same region (*17*–*19*). Fossil footprints record information within extremely narrow spatiotemporal scales (e.g., tens of square meters over periods of hours to days), allowing us to test hypotheses about hominin locomotion, behavior, and environmental context that are inaccessible with skeletal fossils (*20*). By applying new analytical techniques (*21*) to the growing sample of East Turkana footprint sites, we consistently find evidence for two different patterns of hominin foot kinematics. These patterns occur adjacent to each other on the same surfaces and are recorded across multiple sites. Our results offer (i) direct evidence of differing locomotor kinematics among early Pleistocene hominins and (ii) a spatially and temporally limited snapshot of data appropriate for monstrating sympatry (on a scale of hours to days), showing that two different hominin taxa repeatedly crossed paths ~1.5 million years ago in lake margin environments.

Site description

Site ET-2022-103-FE22 (abbreviated FE22) was discovered in 2021 in East Turkana Area 103, within the uppermost Kay Behrensmeyer site (KBS) Member of the Koobi Fora Formation (Fig. 1A) (*22*). The track surface presented here is stratigraphically about 10 m below the Elomaling'a Tuff (Fig. 1, B and C), recently dated to ~1.52 million years ago (Ma) (*23*). Tephrostratigraphic correlations (*16*) indicate that this site is slightly older than any hominin footprint sites previously known from the Turkana Basin (*17*–*19*).

The FE22 track-bearing surface was formed on a 32-cm–thick homogeneous silt unit, which is stratified in a 3.5-m–thick sequence of alternating fine sand and silt (Fig. 1D and fig. S1). Throughout the upper 2.5 m, bedding irregularities indicate cross sections of vertebrate tracks (Fig. 1D and fig. S1); at least five likely track surfaces are preserved (TS-1 to TS-5, Fig. 1D). Laminated sandy silt and sand covered and infilled the track surface excavated here (TS-2) and these layers contain vertebrate body fossils, including those of hominins. The lower 1.3 m includes two bivalve-dominated shell beds with root and plant stem structures interpreted as evidence of reed beds. The upper shell bed has dish-shaped sedimentary structures identified as fish nests (*24*). Overlying sediments are ripple- or horizontally laminated sands and silty sands, interbedded with several massive silt and silty clay units, with only one 25-cm–deep cut and fill structure indicating local channeling (Fig. 1D). There are few root traces and no evidence of mud cracking that would indicate prolonged subaerial exposure.

On the TS-2 surface, we uncovered one continuous trackway made by a single hominin individual and three isolated hominin tracks that, based on sizes and orientations, appear to represent three additional, different individuals (Fig. 2; see also supplementary text). The TS-2 surface also includes 61 bird, 30 bovid, and 3 equid tracks. Many bird tracks are unusually large, the largest being 27 cm wide and several others over 20 cm (Fig. 2E). The size and morphology of these tracks are consistent with those of marabou storks, such as the "giant" *Leptoptilos* cf. *falconeri*. Skeletal fossils from that taxon are currently known only from the Pliocene (*25*), but large bird tracks at Okote Member footprint sites are tentatively attributed to this taxon (*26*).

Results and discussion

The FE22 lithofacies represent an aggrading lake margin sequence. The depositional units

---

[1] Department of Biology, Chatham University, Pittsburgh, PA, USA. [2] Department of Human Origins, Max Planck Institute for Evolutionary Anthropology, Leipzig, Germany. [3] Department of Human Evolutionary Biology, Harvard University, Cambridge, MA USA. [4] Department of Paleobiology and Human Origins Program, National Museum of Natural History, Smithsonian Institution, Washington, DC, USA. [5] School of Biological and Environmental Sciences, Liverpool John Moores University, Merseyside, UK. [6] Department of Ecology, Evolution, and Organismal Biology, Brown University, Providence, RI USA. [7] Center for the Advanced Study of Human Paleobiology, The George Washington University, Washington, DC, USA. [8] Department of Earth and Planetary Sciences, Rutgers University, Piscataway, NJ, USA. [9] Department of Anthropology, Rutgers University, Piscataway, NJ, USA. [10] Turkana Basin Institute, Stony Brook University, Stony Brook, NY, USA. [11] Department of Anthropology, Stony Brook University, Stony Brook, NY, USA.
***Corresponding author. Email: kevin.g.hatala@gmail.com**

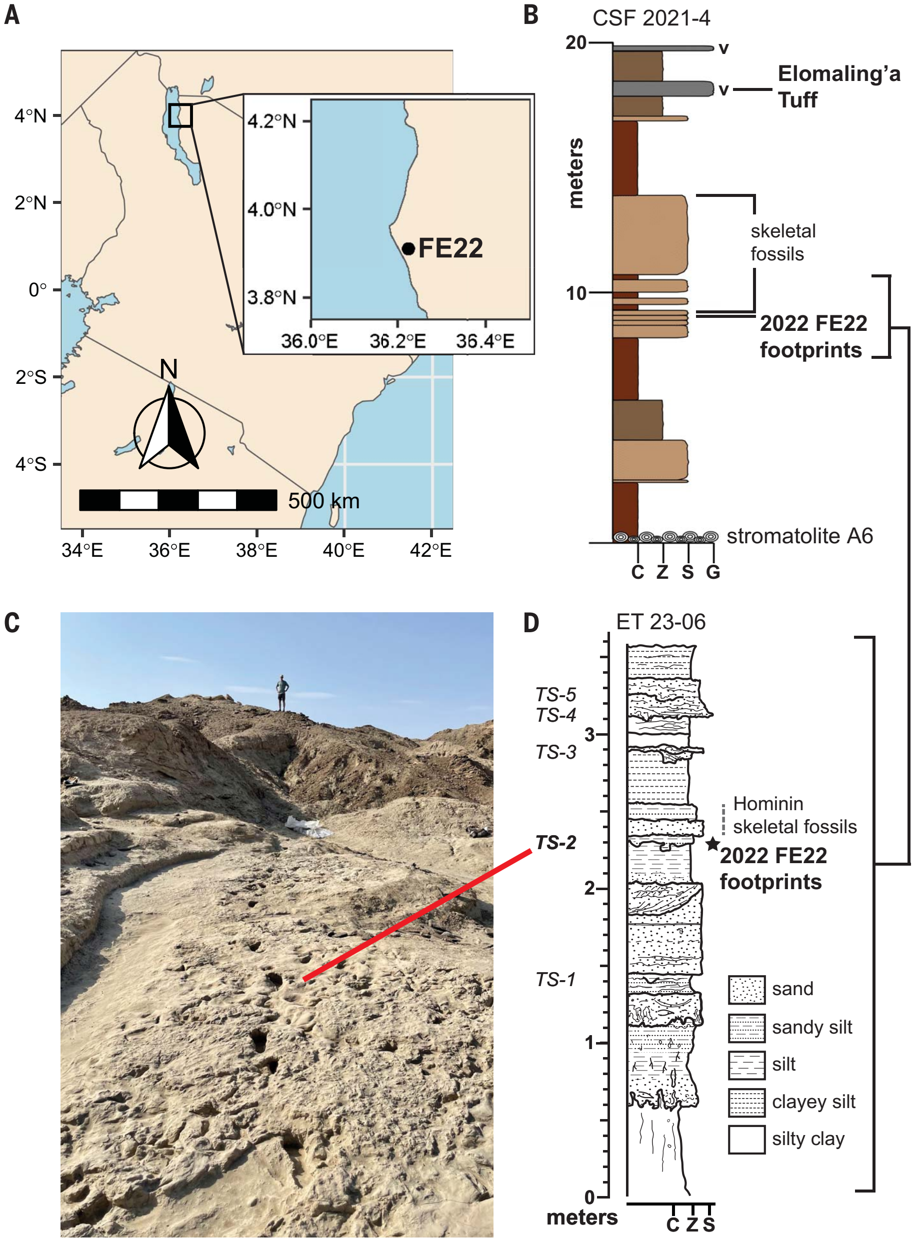

Fig. 1. Context of site ET-2022-103-FE22. (**A**) Map indicating location of ET-2022-103-FE22 in northern Kenya, near the eastern shore of Lake Turkana. (**B**) Geological section showing the general stratigraphic context of the footprint surface and relationship to the Elomaling'a Tuff, dated at 1.52 Ma (*23*). The "v" annotations indicate volcanic tuff layers and horizontal axis labels C, Z, S, and G indicate clay, silt, sand, and gravel, respectively. (**C**) Photograph of TS-2 track surface at site ET-2022-103-FE22, looking approximately north (photo credit: N.T.R.). (**D**) Detailed stratigraphic section of the site showing the location of TS-2 (see also fig. S1). Horizontal axis labels C, Z, and S indicate clay, silt, and sand, respectively. TS indicates levels of track surfaces. TS-2 is <25 cm below sediments from which hominin skeletal fossils were recovered, 10.2 m below the Elomaling'a Tuff. The track surface occurs on a 32-cm–thick silt layer in a sequence of sands and silts. The absence of mud cracking and the presence of mollusc and stromatolite layers in this sequence indicate a shallow subaquatic environment with a stable water table associated with a lake margin (*26*).

(Fig. 1D) record a transition from sedimentation in a stable shoreline with reedbeds to rapid accumulation with minimal sediment reworking, possibly from deposition by a distributary channel on a shallow delta margin. Short hiatuses in sedimentation allowed stabilization of two relatively thick silt beds, one of which formed the TS-2 surface. Animals were walking and standing in shallow water or very close to the shoreline on a wet substrate that was supportive but deformable. After tracks were formed, the surface was gently covered with fine sand and silty sand and preserved under the accumulating strata. There is no evidence for erosion into this surface (e.g., rip-up clasts, coarser basal lag), supporting continuous, rapid sediment accumulation. The lack of mud cracking and rooting indicates that the TS-2 surface was subaqueous or minimally subaerially exposed, and limited overprinting suggests a short time interval between track formation and burial (hours to a few days).

The morphology of the tracks and the information that they retain is partly dependent on the nature of the substrate (*21*, *27*). The TS-2 substrate was soft enough for hominins to sink deeply (~4 cm to 8.5 cm), but cohesive enough to record finely detailed track morphology (figs. S3 to S17). The substrate appears to have been sufficiently stable for hominins to walk at a steady pace. The HT1 trackway is characterized by consistent step lengths (mean 87.28 cm, standard deviation 4.05 cm) and narrow step widths (mean 2.63 cm, standard deviation 3.66 cm). There is no evidence for slipping or other obvious gait perturbations. Based on stride lengths (mean 171.85 cm), we estimate that this individual was moving at about 1.81 m/s, a modestly fast walking pace (*28*). Given the speed and consistency of motion, we assume the HT1 tracks likely represent this individual's normal gait when moving over a soft substrate.

Track depths vary laterally across the TS-2 surface and the isolated tracks all fall within the range of depths observed in the HT1 trackway. With one exception (track HT1-9; fig. S10), the isolated tracks and those within the HT1 trackway all display similar fine morphological details (e.g., ridges between toe impressions; figs. S3 to S17). Their comparable depths and morphological details, combined with their immediate proximity (Fig. 2), make it likely that all hominin tracks were made under similar substrate conditions. Importantly, our analyses account for the ways in which track morphology varies with track depth, allowing tracks of different depths to be compared.

The foot kinematics recorded by the TS-2 tracks were evaluated using methods developed from biplanar x-ray studies of how track morphology is shaped by foot motion (*29*). Previous work has shown that the longitudinal arching of human tracks, quantified as relative arch volume (RAV), is the product of modern human heel-sole-toe rollover kinematics (*21*). Human tracks follow a distinctive pattern wherein RAV increases logarithmically with a track's relative depth (depth scaled to track size). Changes to foot motion and substrate resistance cause humans to make more highly arched tracks as they sink more deeply. Comparisons of RAV, in the context of relative depth, allow for the detection of different kinematic patterns expressed in fossil hominin tracks (*21*). Two of the isolated TS-2 tracks (H2 and H3) have

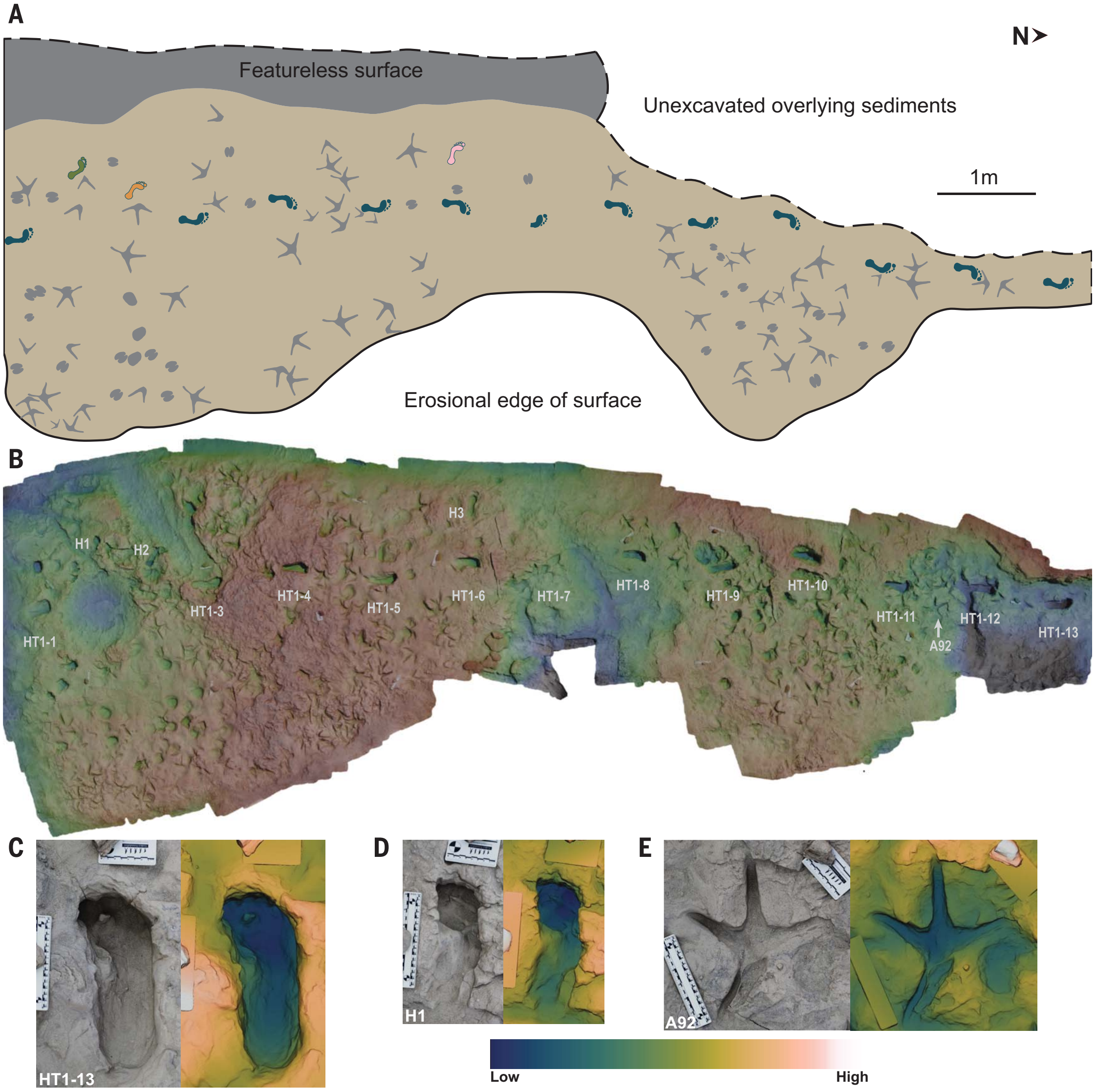

Fig. 2. The TS-2 track surface and selected individual tracks. (**A**) Schematic map of the TS-2 surface. The continuous HT1 trackway appears in dark blue. Isolated tracks H1 (green), H2 (orange), and H3 (pink) are oriented nearly perpendicular to the HT1 trackway. (**B**) Complete 3D model of the TS-2 surface. The isolated tracks (H1 to H3) and the HT1 trackway (HT1-1 to HT1-13) are labeled, as is the bird track (A92) from (E). The original color of the photogrammetric model is blended with a height map (height map spans 30 cm from blue to red). (**C**) Standard image (left) and height map (right) of track HT1-13. (**D**) Standard image (left) and height map (right) of H1, a track smaller than those within the HT1 trackway, oriented in a different direction. (**E**) Standard image (left) and height map (right) of A92, a large bird track. Images in (C) to (E) include the same 15-cm and 8-cm scale bars and are resized to similar scale to facilitate comparisons. Height maps span 13, 9, and 8 cm, respectively, from blue to white.

human-like RAV values for their depth and therefore show evidence of human-like foot kinematics (Fig. 3). The HT1 trackway shows evidence of a different kinematic pattern. These tracks are much flatter for their depth, making them similar in this respect to ~3.66 Ma tracks from Laetoli, Tanzania (Fig. 3). However, many of the HT1 tracks are oppositely pitched from the Laetoli tracks (i.e., deeper forefoot compared with heel impressions), perhaps indicating heel strike and/or push-off patterns that differed not only from those observed in modern humans but also from those evidenced at Laetoli (*21*). Within our comparative sample of 340 modern human tracks (which includes multiple populations making footprints across multiple substrates), the probability of sampling a set of at least five footprints from the same person, which falls this far from the human RAV-relative depth logarithmic regression line, is zero (*22*).

When looking broadly at the entire known sample of ~1.4- to 1.6-Ma East Turkana hominin footprints, we now recognize further evidence for two different patterns of bipedal kinematics. One subset of tracks recovered near Ileret, Kenya (*18*, *19*, *30*) has RAV values that fall within the 95% prediction interval of the modern human RAV-relative depth regression. A second subset has RAV values well outside of that prediction interval, and these are similar to those from the TS-2 HT1 trackway (Fig. 3). One quantifiable track from GaJi10 (*17*), which is close to FE22 but at a higher stratigraphic level, also shows a low RAV similar to those of the HT1 trackway (Fig. 3). Our prior work demonstrated that the longitudinal track arching captured by RAV is generated primarily through heel-sole-toe rollover patterns and deviations from the RAV-relative depth trend observed in modern humans indicate different foot kinematics (which may be coupled with differences in foot anatomy) (*21*). Evaluation of all available evidence from ~1.4- to 1.6-Ma East Turkana sites suggests that two different patterns of locomotor kinematics are recorded on the same footprint surfaces, with some trackways indicating modern human-like locomotion and others representing a different pattern of foot motion.

In addition to the kinematic differences implied by RAV, hallux impressions within the HT1 trackway point toward differences in foot anatomy and/or function when compared with modern human footprints. In absolute value, hallucial abduction angles measured from the HT1 footprints tend to exceed those observed among modern human tracks (Fig. 4A) (*22*). The same is true for the Laetoli G1 trackway, although neither approaches the highly abducted hallux impressions of chimpanzee tracks. In addition to being more abducted, the hallucial orientations within the HT1 trackway are more variable than those of modern human tracks.

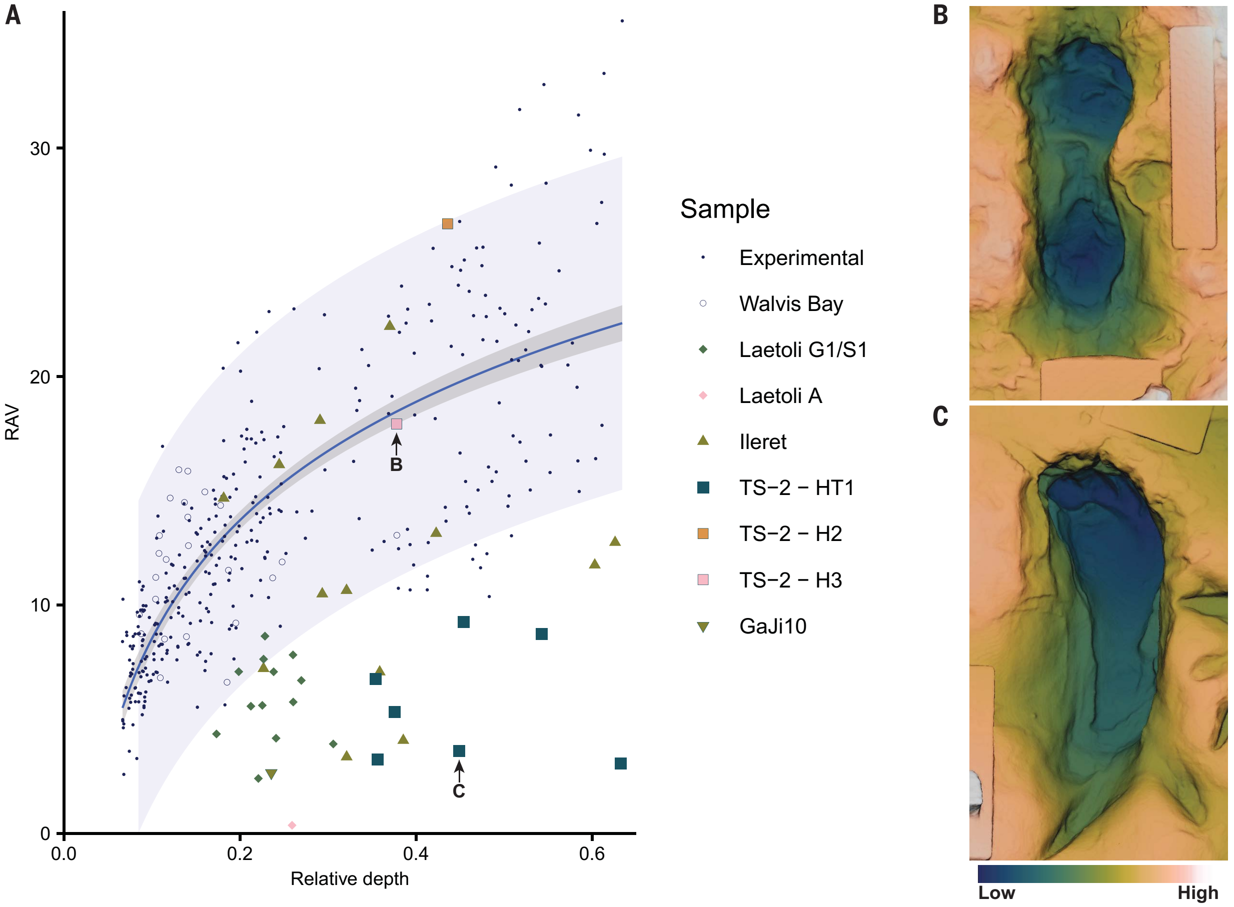

Fig. 3. Patterns of arching among modern experimental and fossil tracks. (**A**) Scatterplot of human and fossil tracks showing relative depth values versus relative arch volume (RAV). The 95% prediction interval (PI) from the modern human RAV-relative depth logarithmic regression is shaded in light blue [regression line in dark blue with 95% confidence interval (CI) in gray]. Tracks from the TS-2 HT1 trackway fall well below the modern human 95% PI, as do some tracks from Ileret, an isolated track from site GaJi10, and most tracks from Laetoli. By contrast, two isolated tracks from TS-2 (H2 and H3) fall within the modern human 95% PI, as do some tracks from Ileret and all ~400- to 500-year-old human tracks from Walvis Bay, Namibia (*22*). Tracks from (B) and (C) are labeled. (**B**) Track H3, which has a RAV of 17.93 at a relative depth of 0.38. (**C**) Track HT1-5, which has a RAV of 3.62 at a relative depth of 0.45. Height maps in (B) and (C) span 8 and 15 cm, respectively, from blue to white.

When comparing mean-centered hallucial abduction across groups, the HT1 sample spans a broader range than modern humans, showing greater variability in step-to-step positioning of the hallux (Fig. 4B). The differences between maximum and minimum abduction angles measured from footprints within the HT1 trackway (15.9 degrees for the left foot, 19.1 degrees for the right foot) fall outside 95% confidence limits derived from iterative resampling of experimental modern human footprints (1.4 degrees to 10.6 degrees) (*22*). Comparable variation in hallucial abduction is observed in Laetoli G1 and chimpanzee footprints (Fig. 4B), but the HT1 and Laetoli G1 tracks are distinct from those of chimpanzees. At HT1 and Laetoli G1, the hallux abducts from the long axis of the foot at the first metatarsophalangeal joint, whereas in chimpanzee tracks abduction initiates at the tarsometarsal joint. Based on track morphology, we hypothesize that the makers of the HT1 and Laetoli G1 tracks differed from modern humans (and chimpanzees) in morphology and/or kinematics at the first metatarsophalangeal joint. Similar hallucial abduction patterns are evident at ~1.5-Ma hominin footprint sites near Ileret (fig. S2; see also supplementary text).

Assuming that our analyses appropriately account for potential substrate variation (*22*), the patterns of track morphology at FE22 might be explained by one early Pleistocene hominin taxon having much greater intraspecific variation in foot anatomy and walking kinematics than that observed in modern humans (*27*). However, the evidence presented above and the skeletal fossil data described below lead us to propose that the TS-2 surface records the co-occurrence of two different taxa, exhibiting different foot morphology and kinematics, within the growing number of early Pleistocene track assemblages at East Turkana.

Despite a sparse record of confidently attributed skeletal fossils, postcranial morphology has been used to infer locomotor variation among early Pleistocene hominin taxa. Robinson (*31*) analyzed lower limb fossils from southern Africa attributed to *Paranthropus* and inferred a locomotor pattern distinct from contemporaneous hominins (*32*). Analyses of early Pleistocene talar fossils from East Turkana and Olduvai Gorge in Tanzania identified morphological differences hypothesized to reflect different patterns of bipedalism in *Paranthropus* and *Homo* (*33*, *34*). More recent studies of pedal fossil morphology have applied three-dimensional (3D) methods, used novel analytical approaches, and incorporated more recently discovered fossils. These continue to highlight an emerging picture of locomotor diversity among early Pleistocene hominins. For example, variable heel strike patterns have been hypothesized based on calcaneal morphology (*35*),

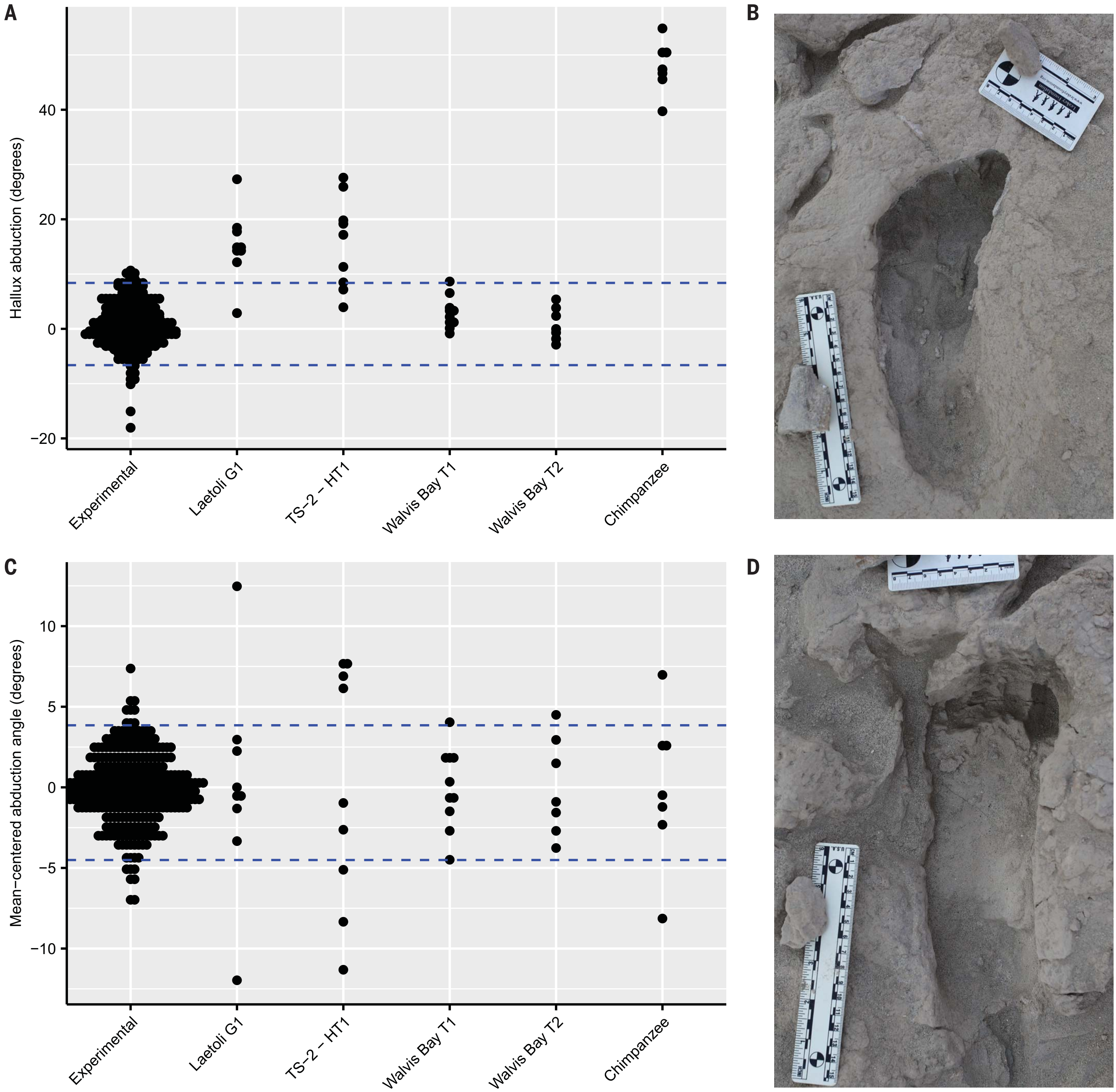

Fig. 4. Hallucial abduction angles among modern experimental and fossil tracks. (**A**) Dotplot showing raw hallucial abduction angles among several track samples. Dashed blue lines indicate the 95% CI of abduction angles from modern human tracks. The TS-2 HT1 tracks and those from Laetoli G1 span well above the upper bound of the modern human 95% CI but their hallux impressions are not nearly as abducted as those of chimpanzee tracks. Abduction angles measured from ~400 to 500-year-old human tracks at Walvis Bay fall almost exclusively within the modern human 95% CI. (**B**) Track HT1-8, with a relatively high hallucial abduction angle (19.18 degrees). Scale bars are 15 cm and 8 cm (photo credit: K.G.H.). (**C**) Dotplot showing mean-centered hallucial abduction angles, to compare variation within samples. Again, dashed blue lines represent the modern human 95% CI. The TS-2 HT1, Laetoli G1, and chimpanzee tracks all span ranges broader than the modern human 95% CI. The Walvis Bay tracks fall almost exclusively within the human 95% CI. This highlights greater step-to-step variation in hallux orientation within the TS-2 HT1 trackway (and Laetoli G1). (**D**) Track HT1-12, with a relatively low hallucial abduction angle (3.94 degrees). Scale bars are 15 cm and 8 cm. HT1-8 and HT1-12 are similarly deep (relative depths of 0.43 and 0.45, respectively; photo credit: K.G.H.)

whereas variation in rearfoot and midfoot kinematics and longitudinal arch anatomy have been inferred from talar morphology (*36*, *37*). Differences in push-off kinematics have been hypothesized based on metatarsal robusticity (*38*). Taken together, the morphologies of known skeletal fossils suggest considerable variation in early Pleistocene hominin foot function (*15*, *39*). These morphological differences are consistent with our finding of two kinematically distinct gaits recorded by early Pleistocene hominin tracks.

Directly relevant to our analyses, first metatarsal base morphology in presumed *Paranthropus* fossils has been linked to greater hallucial abduction than observed in modern humans (*40*). Dorsal narrowing of the first metatarsal head has been found to differentiate *Paranthropus* first metatarsals from those of fossil and modern *Homo* (*40–42*). Dorsal narrowing is also observed in first metatarsals of *Australopithecus afarensis* (*43*), the commonly presumed maker of the Laetoli G1 tracks. These studies have inferred that this morphology would cause a different pattern of toe-off than that observed in modern humans. We hypothesize that the morphologies of *Paranthropus* and *Au. afarensis* first metatarsals are linked to a more abducted and more variable position of the hallux during ground contact, and that this kinematic pattern is evident in the TS-2 HT1 and Laetoli G1 tracks. Based on this, we hypothesize that the HT1 trackway was created by *P. boisei* and the isolated TS-2 tracks by *H. erectus* (*44*).

The co-occurrence of different hominin track morphologies, and their association with other mammal and bird tracks on the TS-2 surface, was geologically instantaneous. The FE22 lithofacies are similar to those of other track-bearing deposits in Area 103 (*17*) and Ileret Area 1A (*18*, *19*), which occur at different stratigraphic levels between ~1.4 and 1.6 Ma. Based on these data, it is clear that hominins were repeatedly visiting lake margin habitats, walking on wet substrates, wading into shallow water, and potentially interacting with other animals frequenting these environments.

Skeletal fossils of *H. erectus* and *P. boisei* have long been known to co-occur within the same geological members of the Koobi Fora Formation (*8*). Prior analyses have shown that fossils of one taxon or the other are more common in certain paleoenvironments (*5*). Lake margin sediments preserve *Homo* and *Paranthropus* fossils at roughly even frequencies, suggesting that these environments may have supported ecological sympatry. However, skeletal fossil assemblages represent time- and space-averaged data and are subject to postmortem displacement and thus are not ideal for evaluating this hypothesis (*6*). Fossil footprints, by contrast, provide focused in situ snapshots that allow interspecific co-occurrences and interactions to be inferred more directly (*6*, *20*, *45*).

At FE22 and at site FwJj14E near Ileret (*18*, *19*, *30*), we have documented two distinct patterns of hominin track morphology on the same footprint surfaces. We propose that these represent two different taxa, characterized by disparate foot anatomies and locomotor kinematics. This interspecific co-occurrence, within meters and hours to days of each other, implies that *H. erectus* and *P. boisei* coexisted and potentially interacted with each other in lake margin environments during the early Pleistocene. Furthermore, given different locations (~40 km apart) and depositional and temporal differences between sites recording these two hominin track morphologies within the same ~200-thousand-year time interval, evidence is provided for a sustained pattern of hominin sympatry. Presumably the lake margin and deltaic environments where the co-occurring tracks are recorded as well as the larger surrounding ecosystems offered resources that were accessible and desirable to both taxa despite apparent adaptive differences. If such sympatry between *Homo* and *Paranthropus* persisted since earlier in time, perhaps since the origins of the genus *Homo* at ~2.8 Ma (*46*), we hypothesize low to neutral competition between these genera. This scenario seems plausible given their apparent adaptations for consuming different dietary resources (*9–13*). Later, climate-caused environmental shifts could have changed the balance of resource availability (*3*), leading to increased competition and potentially driving adaptive shifts toward the riskier, higher-reward food acquisition strategies that later defined our genus (*13*, *47*, *48*). Testing such hypotheses will require detailed analyses of multiple environmental and behavioral data sources and will benefit from integrating fossil footprints with other fossil and archaeological evidence.

REFERENCES AND NOTES

1. B. Wood, E. K. Boyle, *Am. J. Phys. Anthropol.* **159** (suppl. 61), S37–S78 (2016).
2. B. Wood, M. Collard, *Science* **284**, 65–71 (1999).
3. S. C. Antón, R. Potts, L. C. Aiello, *Science* **345**, 1236828 (2014).
4. A. K. Behrensmeyer, *Paleobiology* **8**, 211–227 (1982).
5. A. K. Behrensmeyer, *L'environment Des Hominides Au Plio-Pleistocene*, Y. Coppens, Ed. (Foundation Singer-Polignac, 1985), pp. 309–324.
6. J. T. Faith *et al.*, *Trends Ecol. Evol.* **36**, 797–807 (2021).
7. B. Wood, M. Leakey, *Evol. Anthropol.* **20**, 264–292 (2011).
8. R. E. F. Leakey, A. C. Walker, *Nature* **261**, 572–574 (1976).
9. A. L. Smith *et al.*, *Anat. Rec.* **298**, 145–167 (2015).
10. T. E. Cerling *et al.*, *Proc. Natl. Acad. Sci. U.S.A.* **108**, 9337–9341 (2011).
11. D. B. Patterson *et al.*, *Nat. Ecol. Evol.* **3**, 1048–1056 (2019).
12. P. W. Lucas, P. J. Constantino, B. A. Wood, *J. Anat.* **212**, 486–500 (2008).
13. D. M. Bramble, D. E. Lieberman, *Nature* **432**, 345–352 (2004).
14. S. C. Antón, E. R. Middleton, *J. Hum. Evol.* **179**, 103307 (2023).
15. J. DeSilva, E. McNutt, J. Benoit, B. Zipfel, *Am. J. Phys. Anthropol.* **168**, 63–140 (2019).
16. F. H. Brown, B. Haileab, I. McDougall, *J. Geol. Soc. London* **163**, 185–204 (2006).
17. A. K. Behrensmeyer, L. F. Laporte, *Nature* **289**, 167–169 (1981).
18. M. R. Bennett *et al.*, *Science* **323**, 1197–1201 (2009).
19. K. G. Hatala *et al.*, *J. Hum. Evol.* **112**, 93–104 (2017).
20. K. G. Hatala, N. T. Roach, A. K. Behrensmeyer, *Evol. Anthropol.* **32**, 39–53 (2023).
21. K. G. Hatala, S. M. Gatesy, P. L. Falkingham, *Nat. Ecol. Evol.* **7**, 32–41 (2023).
22. Materials and Methods are available as Supplementary Materials.
23. S. Mana, S. Hemming, D. V. Kent, C. J. Lepre, *Front. Earth Sci.* **7**, 230 (2019).
24. C. S. Feibel, *J. Paleontol.* **61**, 130–134 (1987).
25. D. J. Field, *J. Hum. Evol.* **140**, 102384 (2020).
26. N. T. Roach *et al.*, *Sci. Rep.* **6**, 26374 (2016).
27. S. A. Morse *et al.*, *Am. J. Phys. Anthropol.* **151**, 265–279 (2013).
28. H. L. Dingwall, K. G. Hatala, R. E. Wunderlich, B. G. Richmond, *J. Hum. Evol.* **64**, 556–568 (2013).
29. K. G. Hatala, S. M. Gatesy, P. L. Falkingham, *Interface Focus* **11**, 20200075 (2021).
30. K. G. Hatala *et al.*, *Sci. Rep.* **6**, 28766 (2016).
31. J. T. Robinson, *Early Hominid Posture and Locomotion* (Univ. of Chicago Press, 1972).
32. We include skeletal fossils attributed to *Paranthropus robustus* in a generalized discussion of *Paranthropus* foot anatomy. They are included because of compelling arguments that *Paranthropus* represents a monophyletic group (*49*) and because other studies have noted several morphological similarities between foot fossils attributed to *P. robustus* and *P. boisei* [reviewed in (*15*)].
33. B. A. Wood, *Nature* **251**, 135–136 (1974).
34. B. A. Wood, *J. Hum. Evol.* **3**, 373–378 (1974).
35. T. C. Prang, *J. Hum. Evol.* **80**, 135–146 (2015).
36. T. C. Prang, *J. Hum. Evol.* **90**, 105–119 (2016).
37. R. Sorrentino *et al.*, *J. Hum. Evol.* **142**, 102747 (2020).
38. B. A. Patel *et al.*, *J. Hum. Evol.* **121**, 147–165 (2018).
39. W. E. H. Harcourt-Smith, L. C. Aiello, *J. Anat.* **204**, 403–416 (2004).
40. D. J. Proctor, *Am. J. Phys. Anthropol.* **143**, 631–637 (2010).
41. R. L. Susman, T. M. Brain, *Am. J. Phys. Anthropol.* **77**, 7–15 (1988).
42. R. L. Susman, D. J. De Ruiter, *J. Hum. Evol.* **47**, 171–181 (2004).
43. P. J. Fernández *et al.*, *Proc. Natl. Acad. Sci. U.S.A.* **115**, 8746–8751 (2018).
44. Although it is plausible that either set of footprints may have been produced by *H. habilis* or *H. rudolfensis*, the last appearance dates of confidently attributed specimens of these taxa currently known from the Koobi Fora Formation are 1.75 Ma and 1.78 Ma, respectively (*1*). Given that stromatolite marker bed A6 appears below the TS-2 track surface, the footprints analyzed here are most likely younger than 1.6 Ma (*50*). The last appearance dates of confidently attributed specimens of *H. erectus* (*sensu lato*) and *P. boisei* in the Koobi Fora Formation are 1.44 Ma and 1.41 Ma, respectively (*1*). Based on this premise, it is most parsimonious to hypothesize attribution of the tracks to these two taxa.
45. D. Bustos *et al.*, *Sci. Adv.* **4**, eaar7621 (2018).
46. B. Villmoare *et al.*, *Science* **347**, 1352–1355 (2015).
47. P. Shipman, A. Walker, *J. Hum. Evol.* **18**, 373–392 (1989).
48. N. T. Roach, M. Venkadesan, M. J. Rainbow, D. E. Lieberman, *Nature* **498**, 483–486 (2013).
49. B. Wood, P. Constantino, *Am. J. Phys. Anthropol.* **134**, 106–132 (2007).
50. C. S. Feibel, C. J. Lepre, R. L. Quinn, *J. Hum. Evol.* **57**, 112–122 (2009).

ACKNOWLEDGMENTS

The authors acknowledge Kenyan government permission granted by the Ministry of Sports, Culture, and the Arts and by NACOSTI permit P/22/18336. The authors also thank all members of the Koobi Fora Research Project for their direct assistance with field research that led to the development of this project. This includes E. Ekapatan, M. Haji, D. Kipkebut, H. Longaye, P. Nasmude, L. Nyakitala, H. Sale, and B. Sila for their assistance with the study of site stratigraphy in 2023. K.G.H., P.L.F., and S.M.G. thank M. Kobayashi for contributions to scripts for generating height maps in Autodesk Maya. **Funding:** This work was funded by the following: National Geographic Society (to L.N.L.); National Science Foundation grant BCS-2335894 (to K.G.H.); National Science Foundation grant BCS-1825403 (to K.G.H. and P.L.F.); National Science Foundation grant BCS-1824821 (to S.M.G.); Turkana Basin Institute (to K.G.H., N.T.R., and A.K.B.); UKRI Frontier Research Grant TRACKEVOL (selected by the European Research Council) (to P.L.F.). **Author contributions:** Conceptualization: K.G.H., N.T.R., and L.N.L. Formal analysis: K.G.H., A.K.B., P.L.F., S.M.G., E.M.W.-H., and C.S.F. Funding acquisition: K.G.H., N.T.R., P.L.F., S.M.G., A.K.B., and L.N.L. Investigation: All authors. Methodology: K.G.H., N.T.R., A.K.B., P.L.F., S.M.G., E.M.W.-H., and C.S.F. Project administration: K.G.H., N.T.R., and L.N.L. Visualization: K.G.H., N.T.R., A.K.B., P.L.F., S.M.G., and C.S.F. Writing – original draft: K.G.H., N.T.R., and A.K.B. Writing – review and editing: K.G.H., N.T.R., A.K.B., P.L.F., S.M.G., E.M.W.-H., C.S.F., and L.N.L. **Competing interests:** Authors declare that they have no competing interests. **Data and materials availability:** All data relevant to the analyses presented here are available in the main text or in the supplementary materials. 3D models of individual

tracks, and of the entire TS-2 track surface, are available on MorphoSource (morphosource.org/projects/000601198).

SUPPLEMENTARY MATERIALS

science.org/doi/10.1126/science.ado5275
Materials and Methods
Supplementary Text
Figs. S1 to S17
Tables S1 to S3
References (*51*–*61*)
Data S1 to S3
Code S1 and S2

Submitted 10 February 2024; accepted 16 September 2024
10.1126/science.ado5275